Living on the edge: the role of Atgolgin-84A at the plant ER–Golgi interface

V. VIEIRA*,‡, C. PAIN* (iD), S. WOJCIK* (iD), T. SPATOLA ROSSI* (iD), J. DENECKE† (iD),
A. OSTERRIEDER*,§ (iD), C. HAWES* & V. KRIECHBAUMER* (iD)

*Plant Cell Biology, Department of Biological and Medical Sciences, Oxford Brookes University, Oxford, U.K.

†Centre for Plant Sciences, School of Biology, University of Leeds, Leeds, U.K.

‡Department of Animal and Plant Sciences, The University of Sheffield, Western Bank, Sheffield, U.K.

§Bioethics and Engagement, Mahidol Oxford Tropical Medicine Research Unit (MORU), Centre for Tropical Medicine and Global Health, Nuffield Department of Medicine, University of Oxford, Oxford, U.K.

Summary

The plant Golgi apparatus is responsible for the processing of proteins received from the endoplasmic reticulum (ER) and their distribution to multiple destinations within the cell. Golgi matrix components, such as golgins, have been identified and suggested to function as putative tethering factors to mediate the physical connections between Golgi bodies and the ER network. Golgins are proteins anchored to the Golgi membrane by the C-terminus either through transmembrane domains or interaction with small regulatory GTPases. The golgin N-terminus contains long coiled-coil domains, which consist of a number of α-helices wrapped around each other to form a structure similar to a rope being made from several strands, reaching into the cytoplasm. In animal cells, golgins are also implicated in specific recognition of cargo at the Golgi. Here, we investigate the plant golgin Atgolgin-84A for its subcellular localization and potential role as a tethering factor at the ER–Golgi interface. For this, fluorescent fusions of Atgolgin-84A and an Atgolgin-84A truncation lacking the coiled-coil domains (Atgolgin-84AΔ1-557) were transiently expressed in tobacco leaf epidermal cells and imaged using high-resolution confocal microscopy. We show that Atgolgin-84A localizes to a pre-*cis*-Golgi compartment that is also labelled by one of the COPII proteins as well as by the tether protein AtCASP. Upon overexpression of Atgolgin-84A or its deletion mutant, transport between the ER and Golgi bodies is impaired and cargo proteins are redirected to the vacuole.

Correspondence to: Verena Kriechbaumer, Plant Cell Biology, Department of Biological and Medical Sciences, Oxford Brookes University, Oxford OX3 0BP, U.K. Tel: +44(0)1865488403; e-mail: vkriechbaumer@brookes.ac.uk

Introduction

The eukaryotic cell contains a highly complex network of membrane-bound organelles vital for the synthesis, modification, quality control and packing of proteins, lipids and polysaccharides into transport vectors to mediate either secretion or intracellular accumulations (Vitale & Denecke, 1999). This endomembrane system, also known as secretory pathway, plays diverse roles in cell growth, polarity and development, stress responses and protein storage. A better understanding of the endomembrane system in plants can drive improvement in food production and plant-based products with medicinal, nutritional and commercial value. The plant endomembrane system comprises the endoplasmic reticulum (ER), the Golgi apparatus, the vacuolar system and the plasma membrane. These membrane systems are transiently connected by intermediate compartments: the *trans*-Golgi network (TGN), the prevacuolar compartment or endosome, and the late prevacuolar compartment (Foresti & Denecke, 2008; Foresti *et al.*, 2010; De *et al.*, 2012).

The plant Golgi apparatus is composed of numerous stacks of membrane-bound cisternae, each of which constitutes a discrete Golgi body. Golgi bodies are responsible in part for the processing of proteins received from the ER and their distribution to the plasma membrane and other compartments. The plant Golgi apparatus also synthesizes complex polysaccharides for the cell wall, membrane lipids and glycolipids, and is involved in further processing of N-glycans (Schoberer & Strasser, 2011). Golgi morphology is different between kingdoms, and the mechanisms by which this structure and organization is maintained while providing vital functions for the cell is still poorly understood.

In animal cells, the Golgi apparatus has a perinuclear ribbon-like structure around the ER and is mostly stationary. In plants, there are many discrete Golgi bodies and these are

dispersed and motile (Hawes & Satiat-Jeunemaitre, 2005). Plant cells have many Golgi bodies that are physically connected to the ER (Sparkes *et al.*, 2009), and each is composed of stacked, flattened membrane cisternae. In each plant Golgi body, the cisternae are polarized between the *cis*-face, receiving cargo from the ER, and the *trans*-face, sending cargo forward to post-Golgi organelles. Based on resident enzyme activities (Schoberer & Strasser, 2011), each Golgi stack is subdivided into distinct cisternae from the *cis*- to medial- and the *trans*-face to enable compartmentalized modification of substrates (Moore *et al.*, 1991; Andreeva *et al.*, 1998; Hawes *et al.*, 2008). The TGN also functions as the early endosome (Foresti & Denecke, 2008). Fluorescence recovery after photobleaching analyses showed that the integrity of the Golgi apparatus is maintained through remodelling of the cisternae with their membranes being reabsorbed in the ER and subsequently retrieved back to the Golgi stack. It was demonstrated in plant cells that fluorescent protein fusions of integral membrane enzymes distributed to the different cisternae can cycle in and out of the Golgi body within 5 min (Brandizzi *et al.*, 2002; Schoberer *et al.*, 2010). These results support that the Golgi cisternae are remodelled continuously.

Protein trafficking to and from the Golgi body is mediated by coated membranes. Expression of COPII dominant-negative mutants or for example chemical inhibition of COPI allows the study of these different routes. It is known that disrupting any of these routes leads to the reabsorption of Golgi membranes into the ER (Satiat-Jeunemaitre *et al.*, 1996; Andreeva *et al.*, 2000; Saint-Jore *et al.*, 2002; Stefano *et al.*, 2006), which affects not only Golgi membrane integrity but also ER molecular composition. Proteins that have to exit the Golgi body are exocytosed from the cell or are transported to vacuolar compartments. In addition to Golgi-dependent vacuolar trafficking, direct routes from the ER to the vacuole also exist (Hara-Nishimura *et al.*, 1998; Vitale & Denecke, 1999; Chrispeels & Herman, 2000).

Plant Golgi bodies are composed of discrete units of stacked membrane-bound cisternae that are found distributed throughout the cytoplasm of the cell. Interestingly, they move rapidly along the ER network in an actin-dependent way while maintaining their structure during motility. It has been suggested that Golgi bodies may be surrounded by a dense proteinaceous matrix that excludes ribosomes, maintains the structure of individual Golgi bodies and contributes to the transport of proteins through Golgi bodies (Staehelin & Moore, 1995; Hawes, 2005; Lowe, 2011; Xiang & Wang, 2011).

Golgi bodies maintain a physical connection to the plant ER through the function of several putative Golgi matrix components, including the golgin proteins (Gilson *et al.*, 2004; Latijnhouwers *et al.*, 2005; Renna *et al.*, 2005; Latijnhouwers *et al.*, 2007; Matheson *et al.*, 2007; Osterrieder, 2012; Osterrieder *et al.*, 2017). Golgins are commonly found to act as tethering proteins and have been implicated in the organization and maintenance of Golgi stacks (Ramirez & Lowe, 2009). Mammalian golgins are defined by the presence of long coiled-coil domains, as well as attachment to Golgi membranes via their C-termini [either by tail-anchor transmembrane domains (TMDs) or through binding to small GTPases] (Ramirez & Lowe, 2009; Goud & Gleeson, 2010; Munro, 2011). These features allow the golgins to extend over a significant distance into the cytoplasm, which is an ideal characteristic allowing for capturing or tethering of other membranes, such as transport vesicles, Golgi cisternae or cytoskeletal elements (Preisinger *et al.*, 2004; Efimov *et al.*, 2007). This conformation also enables the golgins to form homo- or heterodimers with other golgins, GTPases or soluble SNARE proteins (Sztul & Lupashin, 2006). Several putative golgins have been identified in *Arabidopsis thaliana*, all of which localize to Golgi bodies, and interaction partners have been identified for some of the golgins (Gilson *et al.*, 2004; Latijnhouwers *et al.*, 2005; Renna *et al.*, 2005; Latijnhouwers *et al.*, 2007; Matheson *et al.*, 2007; Osterrieder, 2012).

Among the identified Arabidopsis golgins is Atgolgin-84A (Latijnhouwers *et al.*, 2007; Osterrieder, 2012) (previously termed Golgin Candidate 1, GC1), a homologue of mammalian golgin-84. Golgin-84 is a mitotic phosphoprotein (Diao *et al.*, 2003); it interacts with the mammalian Rab1 protein (Diao *et al.*, 2003; Satoh *et al.*, 2003) and features a cytoplasmic coiled-coil domain and a C-terminal TMD required for Golgi body targeting (Bascom *et al.*, 1999). The overexpression of Golgin-84, the expression of a mutant version and the siRNA-mediated depletion of the protein, results in a disruption of the Golgi ribbon into large cytoplasmic fragments. These fragments still retain their stacked organization but are significantly reduced in size (Diao *et al.*, 2003). In animal cells, there is strong evidence for the involvement of golgin-84 role in vesicle trafficking. Cells lacking golgin-84 have defects in the maturation of certain plasma membrane proteins and an accumulation of intra-Golgi vesicles containing Golgi residents (Sohda *et al.*, 2010). Golgin-84 proteins, as well as several other mammalian golgins, are involved in tethering specific transport vesicles destined for different regions of the Golgi body (Wong & Munro,). In plants, the first studies on Atgolgin-84A found that the protein located mainly to the *cis*-Golgi with a preference for cisternal rims (Latijnhouwers *et al.*, 2007).

Since the initial identification of Atgolgin-84A, the resolution of light microscopy techniques has improved such that *cis*- and *trans*-Golgi compartments can now be distinguished from one another with relative ease. Using these techniques, we can now identify the suborganellar localization of Atgolgin-84A. Furthermore, using highly sensitive variable angle epifluorescence microscopy (VAEM), novel behaviours of Atgolgin-84A can be observed, hinting at the existence of a pre-*cis*-Golgi compartment that plays a key role in correct targeting of proteins for secretion.

Materials and methods

Molecular biology

Fluorescent GFP fusions of full-length Atgolgin-84A and truncated Atgolgin-84A used were published in Latijnhouwers *et al.* (2007). An mCherry fusion for the full-length Atgolgin-84A was created using the previously published pENTR1A clones (Latijnhouwers *et al.*, 2007) using Gateway® cloning technology according to the manufacturer's instructions (Life Technologies). Constructs were cloned into the binary expression vector pB7WGC2-mCherry (Karimi *et al.*, 2005). Constructs were transformed into the *Agrobacterium tumefaciens* strain GV3101::mp90. The following markers were used for colocalization assays and secretion assays: MnSI-mRFP (Schoberer *et al.*, 2019), ST-GFP (Boevink *et al.*, 1998), mRFP-AtCASP (Renna *et al.*, 2005; Latijnhouwers *et al.*, 2007; Osterrieder *et al.*, 2017) and SP-mCherry (Da Costa *et al.*, 2010).

Transient expression of fluorescent protein fusions in tobacco leaf epidermal cells

Transient expression of fluorescent protein fusions in tobacco (*Nicotiana tabacum* SR1 cv Petit Havana) leaves was carried out by Agrobacteria-mediated infiltration as described by Sparkes *et al.* (2006). Transformed agrobacteria are grown overnight at 28°C in LB media with appropriate selective agents and then pelleted by centrifugation (2200 *g*) for 5 min at room temperature. The pellet is then washed once and suspended in an infiltration buffer composer of 5 mg mL^{-1} glucose, 50 mM MES, 2 mM Na$_3$PO$_4$·12H$_2$O acetosyringone. This bacterial solution is appropriately diluted in infiltration buffer to an OD$_{600}$ 0.1 and infiltrated into 5–6 week old tobacco leaves grown at 21°C under greenhouse conditions and then transferred to an incubator and kept at 23°C for 2–4 days prior to imaging.

Stable expression in Arabidopsis plants

Stable Arabidopsis plants were created using the Agrobacteria-mediated floral dip method described by Clough & Bent (1998). Pelleted transformed Agrobacteria were resuspended in solution composed of 5% sucrose, 500 µL L^{-1} Silwet 77. Flowering Arabidopsis stems were dipped into this solution and agitated briefly for up to 1 min, and the whole plant was wrapped in cling film for 24 h. Seeds from the dipped plants were collected and grown on $\frac{1}{2}$ Murashige and Skoog medium with Hygromycin B selection. All imaging was performed in 4–7 days-old T1 seedlings.

Confocal microscopy

Images obtained by confocal microscopy were acquired using the Zeiss LSM 880 AxioObserver with Airyscan using the Zeiss PlanApo x100/1.46 NA oil immersion lens for image and timeseries acquisition. Brefeldin A (BFA) treatments and secretion assays were performed with excitation at 488 nm (GFP) and 561 nm (mCherry) with emission between 489–536 nm and 588–633 nm for GFP and mCherry, respectively. High-resolution imaging of Atgolgin4A localization was performed using the Airyscan detector with GFP and mCherry excitation at 488 and 561 nm, respectively, and emission at 495–550 nm (GFP) and 570–615 nm (mCherry). Additional imaging was performed using a Zeiss Axio-Observer z1 with a x100/1.46 NA oil immersion lens. Sample excitation at 488 nm was accomplished using the attached iLas2 TIRF optical system capable of orbital excitation. Laser power was varied according to sample quality and all timeseries were obtained with an Andor iXon cooled EMCCD camera.

Secretion assay

For the secretion assay by confocal microscopy, the effector (full-length golgin or mutant, respectively) was infiltrated 24 h prior to cargo infiltration and plants were imaged 3 days after cargo infiltration.

Drug treatment

BFA treatment of tobacco leaf samples was carried out as described (Brandizzi *et al.*, 2002). BFA was dissolved in DMSO at 10 mg mL^{-1} and stored at –20°C. Tobacco leaf pieces with an approximate size of 3 × 3 mm were cut and incubated abaxial side down for 30 min–2 h in a freshly prepared 100 µg mL^{-1} BFA working solution at room temperature. To wash out BFA, leaf samples were transferred into a petri dish with distilled H$_2$O, suspended abaxial side down, and incubated for 1–3.5 h at room temperature depending on the protein tested.

Golgi flipping assay

The likelihood of Golgi bodies marked by transiently expressed ST-GFP and GFP-Atgolgin-84AΔ1-557 to flip 90° within a set time period was assessed using confocal microscopy. Timeseries of 11.51 s were collected of both conditions using confocal microscopy and Golgi bodies were scored according to whether the Golgi bodies flipped approximately 90° during that time period.

Golgi body spatial distribution analysis

To quantify the spatial distribution of Golgi bodies throughout tobacco leaf epidermal cells, images of tobacco leaf epidermal cell transiently expressing ST-GFP and GFP-Atgolgin-84A were collected using the VAEM methods described previously. These images were cropped to the largest possible rectangle that contained only visible cell area. The co-ordinates of all
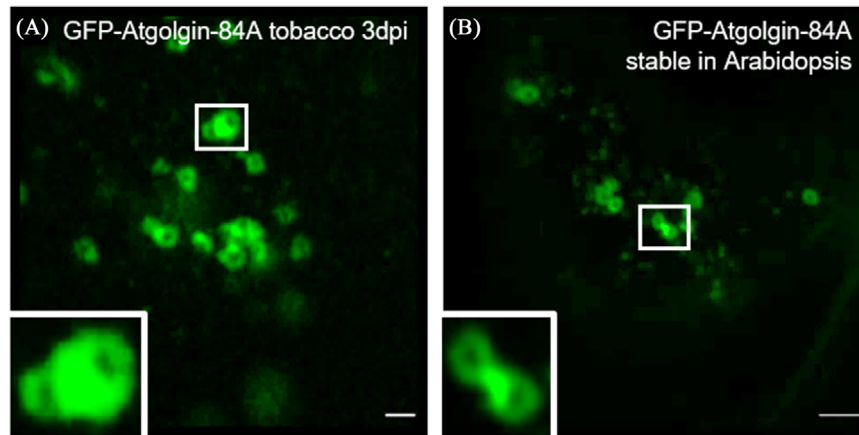
Fig. 1. Expression of GFP-Atgolgin-84A in tobacco and Arabidopsis leaf epidermal cells. (A) GFP-Atgolgin-84A labels ring-shaped structures at 3 dpi. Pairs of Atgolgin-84A rings and accumulation of Atgolgin-84A between ring-shaped structures are frequently observed (inset). (B) GFP-Atgolgin-84A stable expression in Arabidopsis shows localization in ring-shaped structures as in tobacco and pairs of ring-shaped structures are also observed (inset). Scale bars, A = 1 μm, B = 2 μm. Representative images are shown. Biological replicas $n = 5$ with at least five technical repeats each.

Golgi bodies within the image were obtained using the ImageJ multi-point selection tool. The distance between the identified Golgi bodies was analysed in R using the emstreeR (Euclidian spanning tree) package (March *et al.*, 2010) and the tripack package for Delaunay triangulation of points (Renka *et al.*, 2016).

Results

### *Subcellular and suborganellar localization of Atgolgin-84A*

In order to characterize the localization of Atgolgin-84A, the protein was expressed as a fluorescent fusion protein (GFP-Atgolgin-84A) and infiltrated in tobacco leaves. Epidermal cells of infiltrated tobacco plants were imaged with a confocal microscope with Airyscan detector. In plants imaged after 72 h (3 dpi), ring-shaped structures were labelled with rings frequently connected in pairs (Fig. 1A). Upon expression of GFP-Atgolgin-84A, about 20% of Golgi stacks were paired up compared to no Golgi pairs detected in ST-RFP expressing cells ($n = 8$ with 20 Golgi bodies counted for each). In order to confirm the localization observed in tobacco, Arabidopsis Columbia-0 (Col-0) plants were stably transformed with GFP-Atgolgin-84A. As fluorescence was not detected in the T2 generation, leaf epidermal cells of T1 plants were imaged. Stable expression in Arabidopsis shows the same localization pattern as in tobacco plants (Fig. 1B).

VAEM, a method highly sensitive to variation in fluorescence intensity across samples, reveals a nonuniform distribution of GFP-Atgolgin-84A across the observed ring structure. GFP-AtCASP, an ER-Golgi tether that decorates the same ring structures as GFP-Atgolgin-84A, shows an even distribution (Figs. 2A, C and E). GFP-Atgolgin-84A accumulates in specific subregions of the ring-shaped structure (Figs. 2B, D and E).

These regions of high fluorescence consistently localize to the interface of clustering Golgi bodies. This observation was particularly evident in transient overexpression of GFP-Atgolgin-84A in tobacco, where numerous Golgi bodies can be seen forming aggregates of two or more Golgi bodies, which persist despite rapid translocation of these Golgi aggregates through the cytoplasm. The attachment of these Golgi stacks appears to be mediated by the subregions with the highest accumulation of the GFP-Atgolgin-84A (Fig. 2F). These aggregates can also be maintained by the formation of tubular extensions between GFP-Atgolgin-84A rings, with each tubular extension originating and terminating at a point of GFP-Atgolgin-84A accumulation (Fig. 2G). Aggregations of more than two Golgi stacks are also regularly observable, with contact between multiple Golgi bodies maintained by a singular region of high GFP-Atgolgin-84A accumulation (Fig. 2H). Another commonly observed phenomenon in GFP-Atgolgin-84A overexpression is the formation of small tubular extensions attached to individual Golgi bodies. These tubules are capable of elongation and shrinkage and can proceed the movement of Golgi bodies (Fig. 2I) or can trail behind a moving Golgi body. Connections between Golgi bodies can be tubules but also increased fluorescent intensity of GFP-Atgolgin-84A between Golgi body aggregates. When Golgi bodies move apart, these regions of increased intensity appear as tubular connections between the two Golgi bodies (Fig. S1A). When Golgi bodies connected by a tubule move closer together, the tubule between the Golgi shortens until the pair of Golgi bodies is conjoined at a point of relatively increased GFP-Atgolgin-84A fluorescence (Fig. S1B). Thirty-five percent of the tubules are not connected to another Golgi body in the field of view, 20% are observed between pairs of Golgi bodies and 45% of tubules are formed between Golgi body aggregates that are so close together that the connection is not easily observable (Fig. 2J).
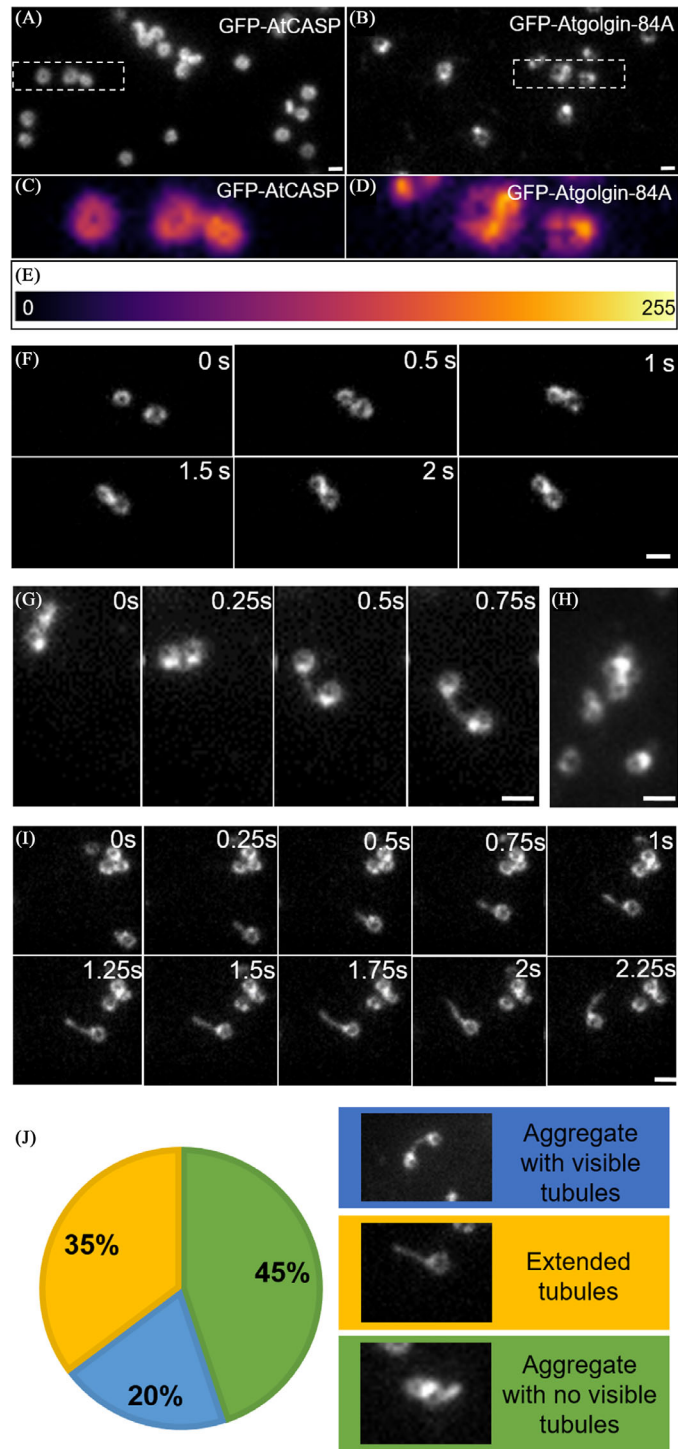
Fig. 2. Characteristics of GFP-Atgolgin-84A transient expression in tobacco. Comparison of the fluorescence distribution of GFP-AtCASP (A) and GFP-Atgolgin-84A (B) when transiently overexpressed in tobacco leaf epidermal cells. White dotted lines mark regions upsampled and magnified (x 3) to provide close ups of GFP-AtCASP structures (C) and GFP-Atgolgin-84A structures (D) pseudocoloured using a modified LUT (E). Scale bars = 1 μm. (F–I) Montages of timeseries capturing common behaviours of GFP-Atgolgin-84A labelled structures, including (F) association of two Golgi bodies by apparent fusion of GFP-Atgolgin-84A rings; (G) connection of Golgi bodies maintained by tubular extensions; (H) the formation of large clusters of multiple Golgi bodies, (I) and tubular extension development independent of Golgi body aggregation. Images collected using VAEM, Scale bars = 2 μm. (J) Golgi tubules are quantitatively characterized in Golgi aggregates with visible tubular connections, tubular extensions with no further Golgi bodies attached and tubules not visible due to aggregation. Biological replicas $n = 3$ with 59 'events' observed.
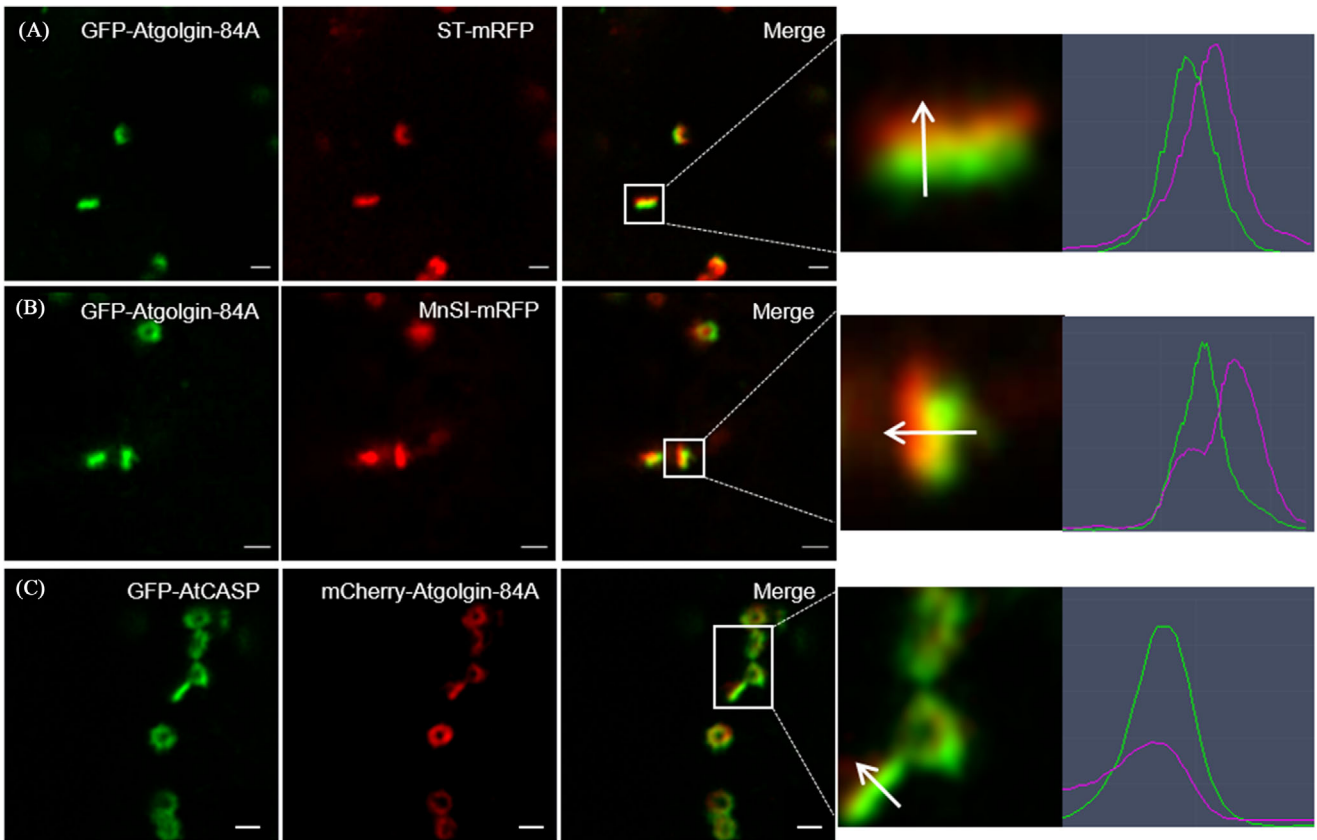
Fig. 3. Coexpression of GFP-Atgolgin-84A and Golgi markers in tobacco plants. (A) Coexpression of GFP-Atgolgin-84A with ST-mRFP, (B) MnSI-mRFP. (C) Coexpression of mCherry-Atgolgin-84A with GFP-AtCASP. Insets show enlarged structures for colocalization. Line profiles indicated by the white arrow show colocalization for Atgolgin-84A and AtCASP but not ST-mRFP or MNSI-mRFP. Scale bars = 1 μm. Representative images are shown. Biological replicas *n* > 10 for every combination with at least five technical repeats each.

Ninety percent of Golgi body aggregates remain stable for the duration of time series imaged (8.5 s). However, when Golgi bodies are found further apart from each other, and connected by tubules, the tubule breaks 29% of the time or forms a tight aggregate 3% of the time (Fig. S2). Therefore, it appears that when Golgi bodies are further apart and connected by a tubule, this connection is more likely to fail. This is most likely due to the separation of the Golgi bodies by the movement of the surrounding cytoplasm and actin cytoskeleton being stronger than the tubular connection. Successful tethering of Golgi bodies by a tubule is a relatively rare event, occurring in 5% of the observed cases. In 53% of cases, the tubule extends from the area of highest GFP-Atgolgin-84A fluorescence and repeatedly retracts and re-extends without forming a connection with another Golgi body. In 42% of cases, the tether retreats into the GFP-Atgolgin-84A ring and does not re-extend for the period observed. In all cases where a tethering event does not occur, the tubule does not come into contact with another Golgi body, instead it extends through the cytoplasm without attaching to another Golgi body and simply collapses (Fig. S3).

In order to characterize its localization in the Golgi body, GFP-Atgolgin-84A is coexpressed using Agrobacterium-mediated infiltration in tobacco plants with various Golgi markers (Fig. 3) starting with the well-described Golgi marker sialyltransferase (ST, Fig. 3A). ST labels the medial/*trans*-Golgi (Munro, 1995; Boevink *et al.*, 1998; Renna *et al.*, 2005). The ring-shaped structures labelled by GFP-Atgolgin-84A and the medial/*trans*-Golgi cisternae labelled by ST-mRFP move together, but the two fluorescent fusion proteins appear to label different Golgi subcompartments (Fig. 3A, inset). Furthermore, the previously described Golgi glycosylation enzyme Golgi-α-mannosidase I (MnSI, Fig. 3B) (Schoberer *et al.*, 2010; Schoberer *et al.*, 2019) located in the *cis*/medial-Golgi stacks is expressed alongside Atgolgin-84A. Atgolgin-84A shows a distinct shift from the *cis*/medial-Golgi enzyme MnSI (Fig. 3B, inset). Colocalization was also tested with the golgin AtCASP (Latijnhouwers *et al.*, 2007; Osterrieder *et al.*, 2017). GFP-AtCASP and mCherry-Atgolgin-84A colocalize (Fig. 3C) placing Atgolgin-84A in a pre-*cis* Golgi compartment.

To test if such a pre-*cis* compartment colocalizes with ER-exit sites (ERES) (Zeng *et al.*, 2015), mCherry-Atgolgin-84A
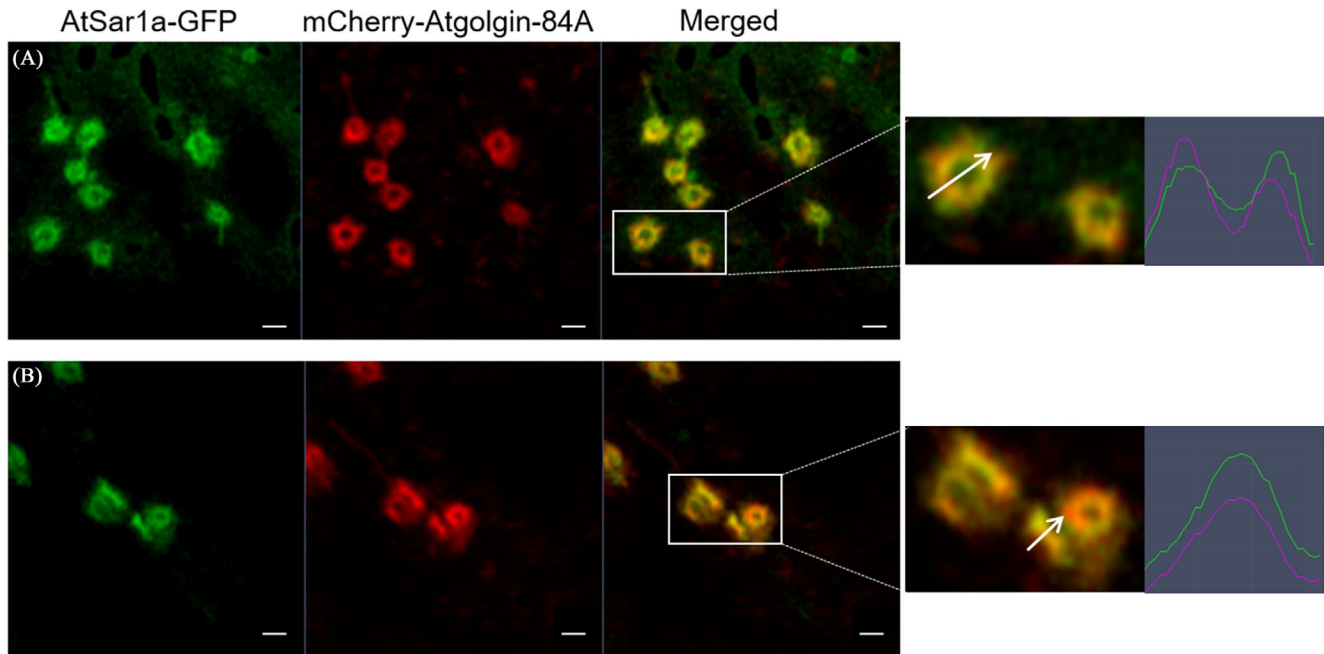
Fig. 4. Coexpression of AtSar1a-GFP and mCherry-Atgolgin-84A in tobacco plants. AtSar1a-GFP is coexpressed with mCherry-Atgolgin-84A. Fluorescence of the two constructs reveals overlapping rings shown in front view (A) as well as imaged sideways (B). Insets show enlargements. Line profiles indicated by the white arrow show colocalization. Scale bars = 1 μm. Representative images are shown. Biological replicas $n = 5$ with at least five technical repeats each.

is coinfiltrated with the ERES marker AtSar1a-GFP (Fig. 4), a GTPase associated with COPII coat formation (Thompson *et al.*, 1994; Wang *et al.*, 2014). Indeed, mCherry-Atgolgin-84A colocalizes with AtSar1a-GFP (Fig. 4A) and no shift between the labels is observed when the cisternae are imaged sideways (Fig. 4B).

Atgolgin-84A overexpression reduces the mean distance between Golgi bodies

As it has been shown that GFP-Atgolgin-84A overexpression can result in the formation of tubular extensions connecting groups of Golgi bodies, the effect of Atgolgin-84A overexpression on the spatial distribution of Golgi bodies was assessed. The mean distance between Golgi bodies marked by either ST-GFP (Fig. 5A) in comparison to Golgi bodies labelled by GFP-Atgolgin-84A or GFP-Atgolgin-84AΔ1-557, respectively, was measured using two methods. In the Euclidian minimum spanning tree method (MST), all Golgi bodies are joined to each other in such a way that the length of the vertices joining the points is minimized (Fig. 5B). In the Delaunay triangulation method (Fig. 5C), all Golgi bodies are joined, yet no point is within the circumcircle of any generated triangle. Both of these methods revealed a significant reduction in the mean distance between Golgi bodies, weighted by the number of Golgi bodies present in each image, marked by overexpression GFP-Atgolgin-84A compared to the over-expression of ST-GFP. Results from four biological repeats with 92 technical repeats of GFP-Atgolgin-84A overexpression and 90 technical repeats of ST-GFP overexpression are shown in Figure 5(D) for MST (Wilcoxon rank sum, p-value $= 3.6 \times 10^{-13}$) and in Figure 5(E) for the Delaunay triangulation (Wilcoxon rank sum, p-value $< 2.2 \times 10^{-16}$). Expression of the deletion mutant GFP-Atgolgin-84AΔ1-557 did not result in such reduction in the mean distance (MST: Wilcoxon rank sum, p-value $= 0.3633$, Fig. 5F; Delaunay triangulation: Wilcoxon rank sum, p-value $= 0.08789$, Fig. 5G).

Atgolgin-84A imaging during Golgi disassembly upon BFA treatment

To gain insight into the behaviour of Atgolgin-84A labelled structures, we studied its response to BFA treatment and compared this response to that of ERES or *cis*-Golgi markers (Osterrieder *et al.*, 2009; Schoberer *et al.*, 2010). To this end, tobacco leaf epidermal cells transiently expressing GFP-Atgolgin-84A, the ERES marker AtSar1a-GFP or the *cis*/medial-Golgi marker, MnSI-mRFP, respectively, were incubated in a BFA solution or DMSO as a control (Figs. 6A–C). If Atgolgin-84A is located at the *cis*-Golgi, a redistribution of the protein into the ER after BFA treatment as shown for the *cis*-Golgi markers (Schoberer *et al.*, 2010) is predicted. MnSI-mRFP relocalizes to the ER network after BFA treatment (Fig. 6D). AtSar1a-GFP labels the
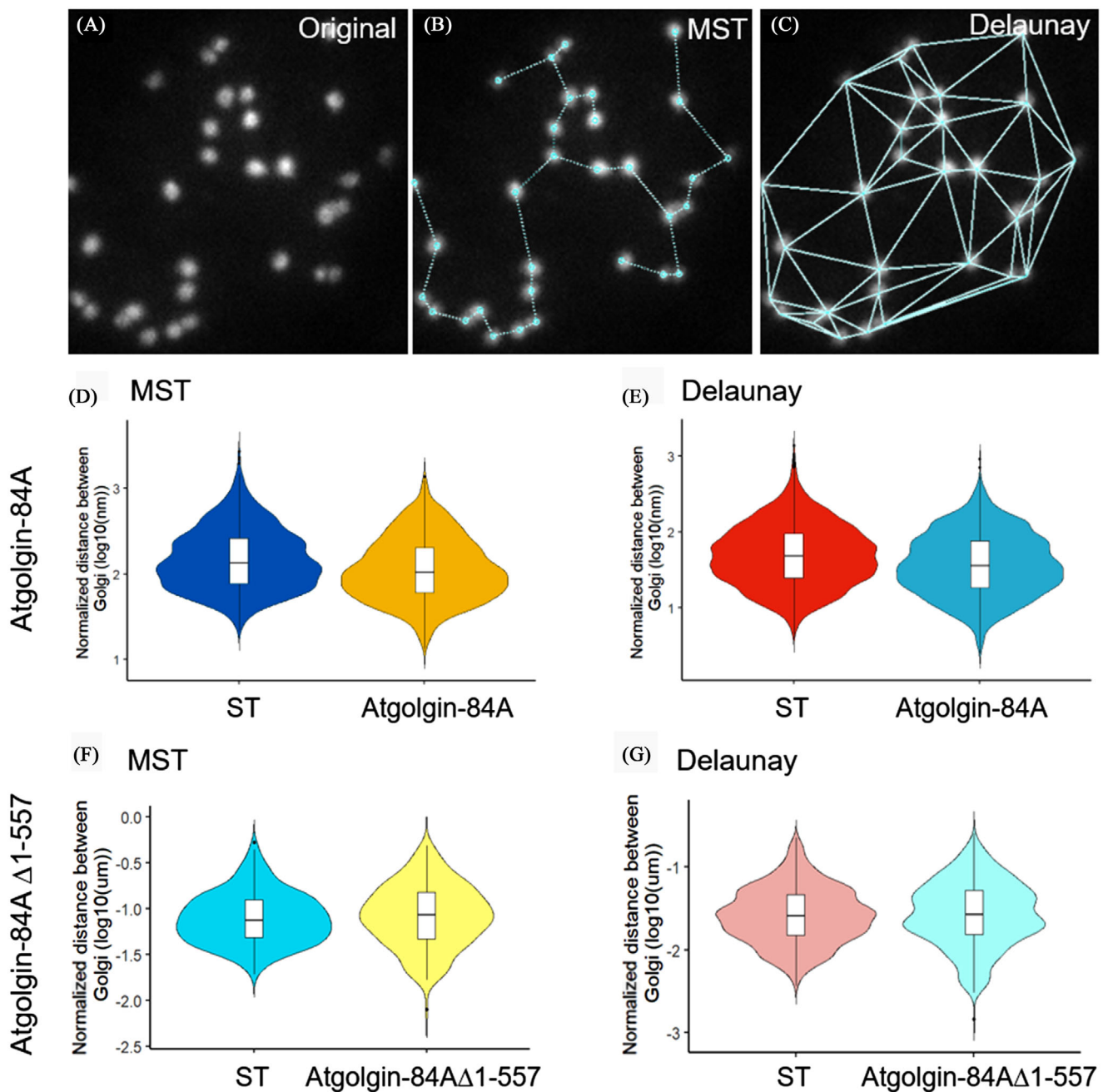
Fig. 5. Mean distance between Golgi bodies upon transient overexpression of ST-GFP and GFP-Atgolgin-84A or GFP-Atgolgin-84AΔ1-557. (A–C) The spatial distribution of Golgi bodies revealed by transient overexpression of ST-GFP (A) with the distance between Golgi bodies calculated either by the MST method (B) or by Delaunay triangulation (C). Calculated distances represented by cyan lines. (D–G) Boxplot comparison of the log mean distance between Golgi bodies (weighted by number of Golgi bodies per image) calculated by using the MST method: GFP-Atgolgin-84A ($n = 3$, 92 cells) compared to ST-GFP ($n = 3$, 90 cells) in D, GFP-Atgolgin-84AΔ1-557 ($n = 2$, 10 cells) compared to ST-GFP ($n = 2$, 10 cells) in F and Delaunay triangulation: GFP-Atgolgin-84A ($n = 3$, 92 cells) compared to ST-GFP ($n = 3$, 90 cells) in E, GFP-Atgolgin-84AΔ1-557 ($n = 2$, 10 cells) compared to ST-GFP ($n = 2$, 10 cells) in G.

cytoplasm and puncta (Fig. 6E). Atgolgin-84A mainly labels puncta after BFA treatment (Fig. 6F) indicating differences in distributional persistence of a golgin and a *cis*-Golgi enzyme (Osterrieder *et al.*, 2009).

Localization of the truncated protein Atgolgin-84AΔ1-557 lacking the long coiled-coil domain

Atgolgin-84A is predicted to have long coiled-coil domains and these are suggested to be the tethering motif in the
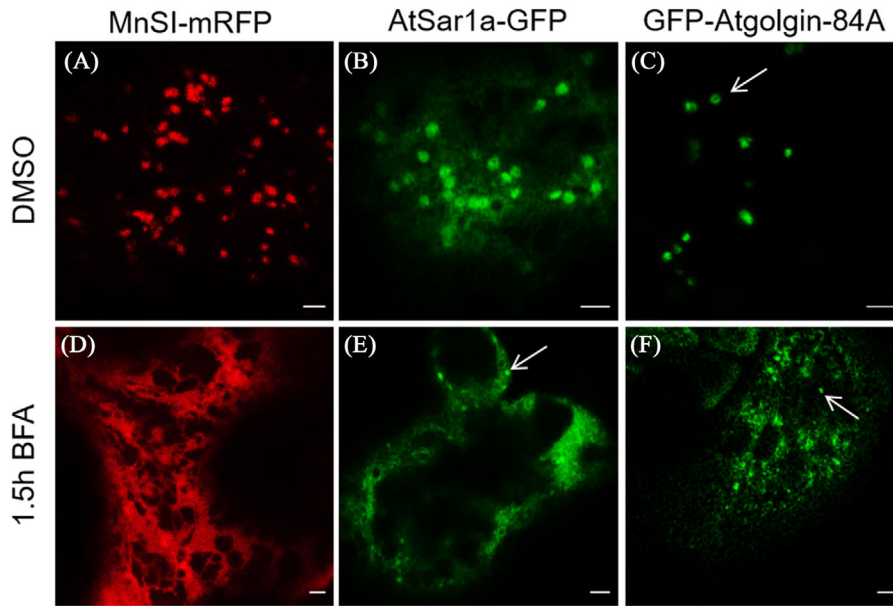
Fig. 6. BFA treatment of tobacco leaves expressing MnSI-mRFP, AtSar1a-GFP or GFP-Atgolgin-84A. Small pieces of tobacco leaves expressing (A) MnSI-mRFP, (B) AtSar1a-GFP and (C) GFP-Atgolgin-84A were incubated in water containing 0.1% DMSO as a control. All three protein fusions labelled Golgi bodies (C, arrow) as seen in nontreated leaves. After incubation in BFA for 1.5 h, (E) AtSar1a and (F) Atgolgin-84A relocalize to the cytoplasm and puncta (E and F, arrows). (D) MnSI-mRFP relocalizes to the ER. Scale bars = 2 μm. Representative images are shown. Biological replicas $n = 3$.

golgin structure (Fig. 7A). In order to investigate the function of the coiled-coil domains, an Atgolgin-84AΔ1-557 construct was obtained by deleting the N-terminal region predicted to be coiled-coil (Latijnhouwers *et al.*, 2007) (Fig. 7B). The Atgolgin-84A deletion mutant comprises the TMD, and approximately 100 amino acids preceding the TMD. This region (amino acids 558–707) is necessary and sufficient for Golgi localization (Latijnhouwers *et al.*, 2007).

GFP-Atgolgin-84AΔ1-557 transiently expressed in tobacco leaf epidermal cells labels ring-shaped structures with pro-

truding tubules (Fig. 8, white arrows). These tubules are capable of elongation and retraction over time. Some of these thin tubules are connecting ring-shaped structures (Fig. 8, yellow arrows), others are mobile and can also show branching (Fig. 8, white arrows).

To investigate the suborganellar localization, mCherry-Atgolgin-84AΔ1-557 was coexpressed with the ERES marker AtSar1a-GFP (Fig. 9). As the full-length version, Atgolgin-84AΔ1-557 colocalizes with the ERES marker indicating similar localization for full-length and truncated proteins.
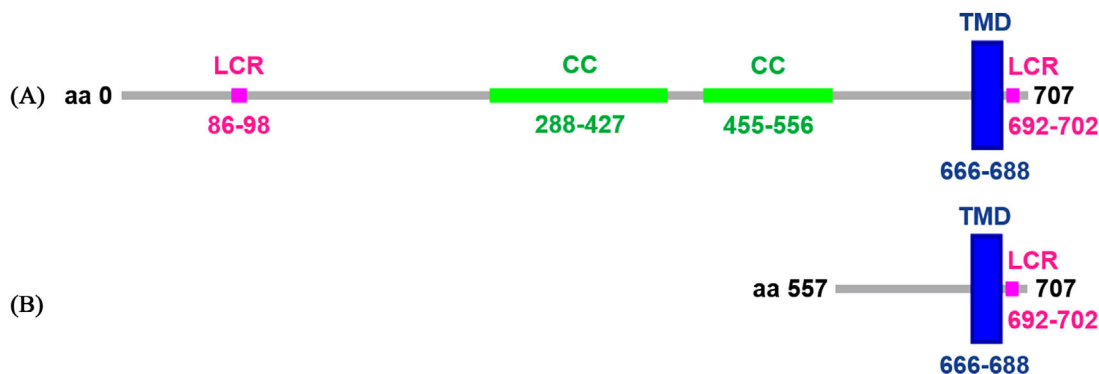
Fig. 7. Schematic representation of the Atgolgin-84A full-length protein and deletion mutant Atgolgin-84AΔ1-557. (A) Predicted structure of the full-length Atgolgin-84A protein featuring two coiled-coil domains (CC, in green), two low complexity regions (LCR, in pink) and a transmembrane domain (TMD, in blue). The TMD at the C-terminus anchors the golgin to the Golgi membrane. (B) Atgolgin-84A deletion mutant containing the TMD and 109 amino acids preceding the predicted TMD.
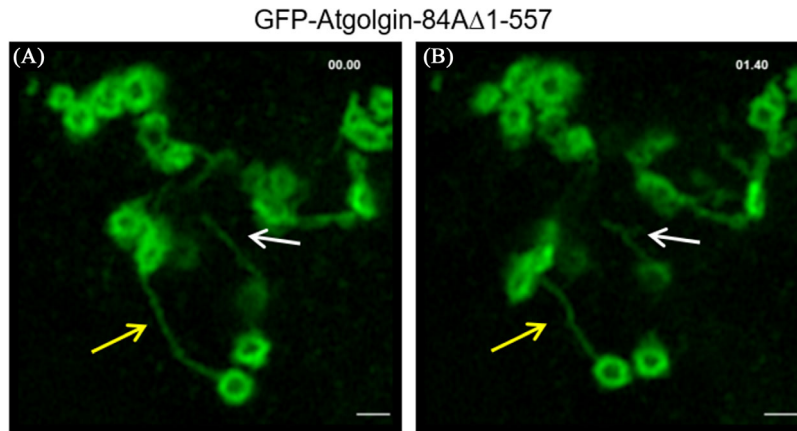
Fig. 8. Time-lapse images of GFP-Atgolgin-84A∆1-557 expression in tobacco leaf epidermal cells. GFP-Atgolgin-84A∆1-557 labels ring-shaped structures with long tubules. Some tubular structures connect several ring-shaped structures (yellow arrows). Tubular structures can elongate and retract and can branch into two tubular structures (white arrows). Scale bars, 1 µm. Time points given in seconds. Representative images are shown. Biological replicas $n = 3$.

*The coiled-coil domain in Atgolgin-84A is involved in Golgi dynamics*

During imaging of Atgolgin-84A∆1-557, it was observed that the ring-shaped structures often flip and turn 90° in respect to the cell surface (Fig. 10A), which is not the case when expressing a Golgi marker, such as ST-GFP alone. This ability to flip sideways by 90° was quantified for ST-GFP and GFP-Atgolgin-84A∆1-557 by counting how many ring-shaped structures flip and do not flip during a time series of 11.51 s (Fig. 10B). When expressing ST-GFP, only 9% (13 out of 140) of Golgi bodies are flipping sideways and 91% were facing forward (Fig. 10B). When GFP-Atgolgin-84A∆1-557 is coexpressed with ST-GFP, 43% of the Golgi bodies (59 out of 136) flip sideways and only 57% are observed facing forward (Fig. 10B).

The effect of overexpression of Atgolgin-84A in protein trafficking

Overexpression of Atgolgin-84A results in Golgi body aggregates and can occasionally cause necrosis in tobacco leaves resembling the locked version of the dominant-negative mutant Sar1-GTP that impairs the trafficking between ER and Golgi (Osterrieder et al., 2009). In addition, compartments labelled by the Atgolgin-84A∆1-557 exhibit long tubular structures. The effects in disrupting the Golgi body either by generating pairs of Golgi bodies or by the induction of long tubules can influence the entry of cargo into the Golgi. To test the hypothesis that Atgolgin-84A influences the rate of protein trafficking, a signal peptide (SP) from the Arabidopsis chitinase fused to mCherry (SP-mCherry) is used as cargo. SP-mCherry has been used before as a marker for the default secretion pathway (Da Costa et al., 2010). SP-mCherry enters the secretory pathway via the SP, and after cleavage of the SP, mCherry is transported to the Golgi apparatus and as it is lacking any other sorting signals by default arrives at the extracellular matrix (Figs. 11A, B). If the overexpression of GFP-Atgolgin-84A or GFP-Atgolgin-84A∆1-557 has an effect on protein transport, SP-mCherry should not accumulate in the apoplast (Fig. 11C). As expected, SP-mCherry alone mainly labels the apoplast with less than 10% of cells
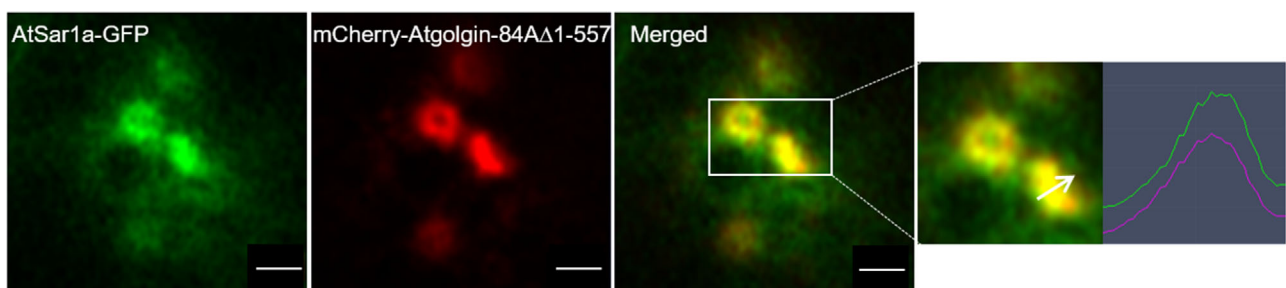
Fig. 9. Coexpression of AtSar1a-GFP and mCherry-Atgolgin-84A∆1-557 in tobacco leaf epidermal cells. AtSar1a-GFP coexpression with mCherry-Atgolgin-84A∆1-557 reveals similar location of both fusion proteins. Inset shows enlargement. Line profiles indicated by the white arrow show colocalization. Scale bars = 1 µm. Representative images are shown. Biological replicas $n = 10$ with at least five technical repeats each.
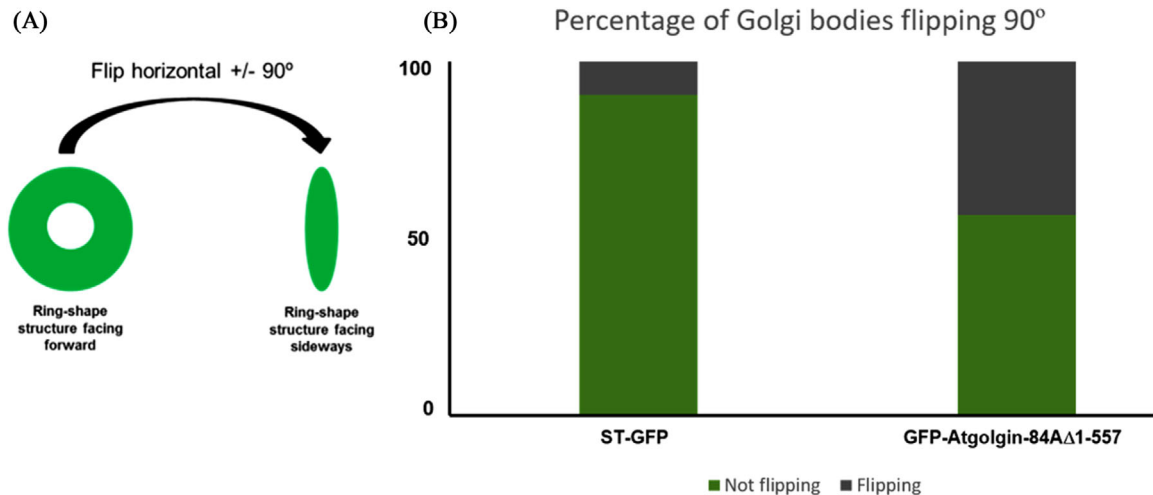
Fig. 10. Analysis of Golgi flipping when expressing ST-GFP alone or with Atgolgin-84AΔ1-557. (A) Schematic representation of Golgi flipping. (B) Bar graph representing the number of Golgi bodies that flip sideways during time series when expressing ST-GFP with or without Atgolgin-84AΔ1-557. Golgi bodies were quantified in two biological replicas; $n \geq 60$ Golgi bodies were assessed per independent experiment.

showing additional vacuolar labelling (Da Costa *et al.*, 2010) (Fig. 11A). Coexpression of SP-mCherry with Atgolgin-84A or Atgolgin-84AΔ1-557 results in the mCherry signal being detected predominantly in the vacuole (Figs. 11D–F). A fraction of SP-mCherry is detected in the apoplast when the truncated golgin construct is expressed (Fig. 11F).

Discussion

### *Atgolgin-84A is located in a pre-*cis-*Golgi subcompartment*

Atgolgin-84A does not colocalize with medial/*trans*- and *cis*-Golgi markers (Figs. 3A, B) but moves together with the Golgi cisternae. Coexpression of Atgolgin-84A with the tethering protein AtCASP (Fig. 3C) and AtSar1a-GFP, a COPII component, labelling ERES, shows colocalization of the constructs (Fig. 4) indicating that Atgolgin-84A is located in a pre-*cis*-Golgi subcompartment. Atgolgin-84A could have a role in tethering COPII components to the Golgi during assembly of the transporters. The ability of golgins, including golgin-84, to tether vesicles in mammalian cells was shown *in vitro* using purified golgins and isolated vesicle fractions (Malsam *et al.*, 2005) as well as in intact cells (Wong & Munro, 2014). Atgolgin-84A and AtSar1a could also label the site of cargo arrival at the Golgi. Such Golgi entry sites have been suggested as sites of protein import and Golgi membranes behave as a single secretory unit moving along the ER (Silva *et al.*, 2004) but do not exclude the existence of isolated ERES with a different machinery.

In coexpression with MnSI-mRFP (Fig. 3B), GFP-Atgolgin-84A was not detected in the centre of the Golgi cisternae, whereas MnSI-mRFP labels the centres of cisterna indicating that Atgolgin-84A could be tethered at the rims of the cister-

nae. Such differences in distribution were previously shown in photobleaching experiments; GFP-tagged glycosylation enzymes, such as mannosidases, were found to diffuse freely without constraints within the Golgi membranes (Schoberer & Strasser, 2011). GFP-Atgolgin-84A is also detected in aggregates with high intensity of fluorescence connecting the ring-shaped structures (Fig. 2H), whereas *cis*-Golgi markers, such as MnSI, do not accumulate in-between the ring-shaped structures (Fig. 3B). Atgolgin-84A accumulates in specific subregions of the ring-shaped structure. These protein accumulations are the contact sites of Golgi pairing as well as tubule extension (Fig. 2). Clustering analysis revealed that overexpression of Atgolgin-84A induces Golgi clustering (Fig. 5). It is hypothesized that Golgi bodies are generated from a pre-existing ones or an ERES (Hawes *et al.*, 2010); hence, golgin overexpression might inhibit the separation of the cisternae and as such cause Golgi clusters. In addition, interactions between the pre-existing Golgi bodies could contribute to the cluster formation.

BFA treatment shows that Atgolgin-84A does not redistribute to the ER and instead stays in puncta that could be the Golgi matrix

Also upon BFA treatment, Atgolgin-84A behaves more like the ERES marker AtSar1a than the *cis*-Golgi marker MnSI (Fig. 6). Atgolgin-84A and AtSar1a-GFP do not redistribute to the ER during BFA treatment as do *cis*-Golgi markers, such as MnSI (Schoberer *et al.*, 2010). Sar1a is only recruited to the ERES during assembly of the transport carrier and therefore remains cytoplasmic when ER and Golgi membranes hybridize in one compartment upon BFA treatment. In comparison, Atgolgin-84A is found in puncta, which could indicate a role in maintaining the Golgi body, acting as a scaffolding
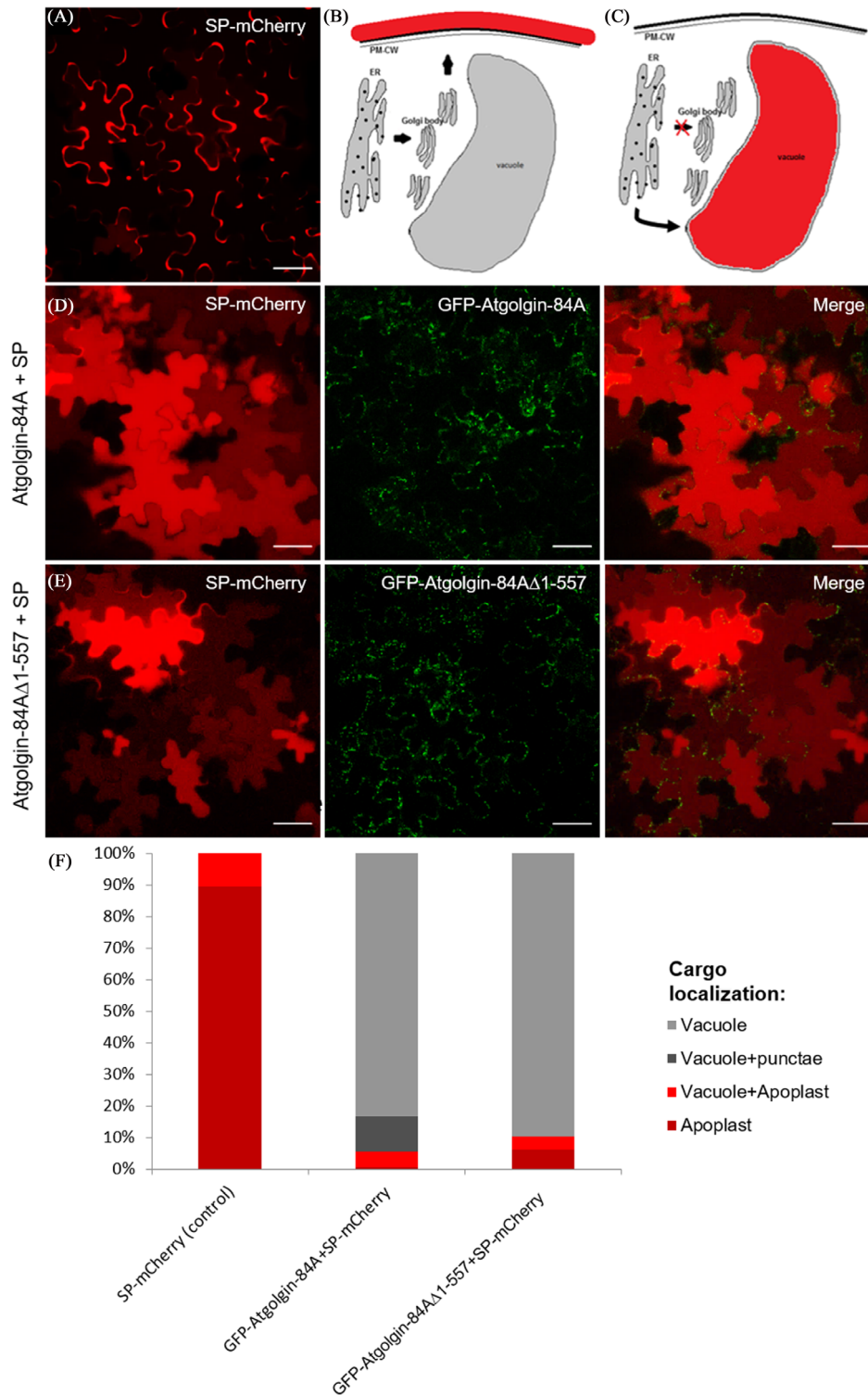
Fig. 11. Secretion assay using transient expression of SP-mCherry in tobacco leaf epidermal cells. (A) All fluorescent fusions were expressed alone as controls: SP-mCherry is detected in the apoplast. GFP-Atgolgin-84A and GFP-Atgolgin-84AΔ1-557 are detected in ring-shaped structures. Schematic diagrams indicate the apoplast localization of SP-mCherry when only SP-mCherry is expressed (B) and the changed SP-mCherry localization upon expression of GFP-Atgolgin-84A o GFP-Atgolgin-84AΔ1-557 (C). Coexpression of SP-mCherry with GFP-Atgolgin-84A (D) or GFP-Atgolgin-84AΔ1-557 (E). Expression of GFP-Atgolgin-84A or GFP-Atgolgin-84AΔ1-557 changes SP-mCherry localization and mCherry is detected predominantly in the vacuole. Scale bars = 50 μm. (F) Quantification of the number of cells showing different labelling by mCherry. Number of cells counted per each different protein expression combination in three biological replicas, technical replicas $n \geq 47$.

linked to other elements of a putative Golgi matrix during bio-genesis. These could represent matrix substructures during re-assembly of the Golgi. A Golgi matrix was suggested in mammalian cells as after detergent-treatment of Golgi membranes a proteinaceous exoskeleton remains that is retaining Golgi structure (Kristen, 1978; Staehelin & Moore, 1995). In plant cells, intercisternal elements and a ribosome-excluding zone around the Golgi body were shown by electron microscopy; this has been suggested to be an equivalent of the Golgi matrix (Kristen, 1978; Staehelin & Moore, 1995). Other proteins to remain in Golgi remnants upon BFA treatment are the SNARE protein AtSYP31 (Witte *et al.*, 2011; Ito *et al.*, 2012; Ito *et al.*, 2018) and the Arabidopsis mannosidase MNS3 (Schoberer *et al.*, 2019).

Atgolgin-84A as an ER tether involved in maintaining Golgi body orientation

Overexpression of the Atgolgin-84A∆1-557 (Figs. 5F, G) did not result in the formation of Golgi aggregates as observed with the full-length protein (Figs. 5D, E), indicating that the coiled-coil domains are necessary for pairing of Golgi bodies. Upon expression of the deletion mutant, an increase of Golgi body flipping and a decrease of Golgi bodies facing forward were observed in comparison with expression of the medial/*trans*-Golgi marker ST-GFP (Fig. 10). One possible explanation for this is that the deleted long coiled-coil domain is responsible for keeping the Golgi body perpendicular to the cell wall and that expression of GFP-Atgolgin-84A∆1-557 could potentially lead to impaired ER-Golgi tethering. Atgolgin-84A could work together with AtCASP to tether ER and Golgi. When a dominant-negative truncation of AtCASP is expressed, the ER and Golgi bodies are still connected, but a gap is visible between both compartments (Osterrieder *et al.*, 2017).

Atgolgin-84A could have a role in protein trafficking

Overexpression of both the golgin GFP-Atgolgin-84A and its truncation results in the redirection of a chitinase SP from the apoplast to the vacuole (Fig. 11). One hypothesis is that both golgin overexpression and the overexpression of a defective truncated protein can disrupt the tether between ER and Golgi and thereby also disrupt ER-Golgi transport and impair trafficking between ER and Golgi. However, further experiments, such as analysis of cargo protein glycosylation, are required to determine at which point in the secretory pathway the SP-mCherry trafficking is disrupted. It is rather unexpected that expression of both full-length and deletion mutant shows similar responses in terms of SP transport. This could be due to titration effects and/or disruption of fine-tuning in transport routes by changes in Atgolgin-84A protein levels in overexpression and a potential dominant-negative effect by the truncated version. It might also be due to Atgolgin-

84A overexpression inducing pairs of Golgi bodies (Fig. 1) and Golgi aggregation (Figs. 5D, E), which could affect the structure of the organelle impairing entry of cargo into the Golgi. Upon overexpression of the deletion mutant protein lacking coiled-coil domains, the distance between ER and Golgi could be increased or the connection between compartments could be loosened preventing proper docking of cargo transporters. All these could compromise Golgi structure leading to the activation of an alternative pathway for cargo export from ER to the vacuole. The fact that ST-mRFP and MnSI-mRFP still reach the Golgi and do not show any ER retention or mistargeting to the vacuoles suggests that ER to Golgi transport is unaffected. However, transport of membrane proteins and soluble proteins is fundamentally different because soluble proteins do not require signals to mediate secretion but they require sorting signals to avoid secretion by default in order to reach vacuoles or other organelles instead. In contrast, Golgi-resident membrane proteins may require specific signals to reach post-Golgi compartments.

If the transport of soluble proteins is compromised, cells could be responding to GFP-Atgolgin-84A overexpression by exporting unnecessary cargo from the ER and send it to the vacuole for degradation (Wang *et al.*, 2018). Trafficking to the vacuole can be either through a Golgi-dependent route or a Golgi-independent route directly from the ER in precursor accumulating vesicles and fuse directly to the protein storage vacuole (Hara-Nishimura *et al.*, 1998; Vitale & Raikhel, 1999; Chrispeels & Herman, 2000). The Golgi-independent route has been described for the plant-specific insert in tobacco cells when the Golgi-mediated route is impaired by the expression of dominant-negative mutant of GTPases, for example, the Sar1-GTP locked version (Pereira *et al.*, 2013; Vieira *et al.*, 2019). The pre-*cis*-Golgi also contains proteins with specific roles in protein sorting (Ito *et al.*, 2018), suggesting that there might be a recognition of cargo before the entry in the *cis*-Golgi body. This could explain the Golgi bypass reported for some vacuole-targeted proteins (Pereira *et al.*, 2013; Vieira *et al.*, 2019).

A hidden ribbon structure: pearls on a string

In plants, dynamic extensions have been observed in a number of different organelles: stromules from plastids, peroxules from peroxisomes and matrixules from mitochondria (Mathur *et al.*, 2012). It is possible that the observed Golgi tubules are not an artefact at all, but that the Atgolgin-84A fusions simply reveal a network of tubular connections that connect individual Golgi bodies. If this can be confirmed independently, it would suggest that plant cells also contain a single Golgi apparatus, except that in plants it is not forming a juxtanuclear cluster as observed in mammalian cells, but covers the entire cell cortex, possibly to supply the cell wall with essential polysaccharides and cell wall proteins.

Interestingly, the tubular extensions protruding from Golgi bodies and connecting individual Golgi bodies observed with Atgolgin-84A fusions are very similar to tubules observed with a newly designed fluorescent fusions of the plant K/HDEL receptor (ERD2) that retains biological activity (Silva-Alvim *et al.*, 2018). The ERD2 gene product was previously shown to exhibit a dual ER-Golgi localization, but this was based on *C*-terminal fusions, which have lost biological activity. The new fusion (YFP-TM-ERD2) is exclusively observed at the Golgi apparatus and in tubular extensions that connect two or more Golgi bodies. It is yet unclear if ERD2 Golgi residency is due to the presence of a very fast ER export signal, or due to a Golgi-retention signal. Golgi retention was shown to be the clue to the apparent insensitivity of MNS3 to BFA-induced redistribution observed for MNS1 and other Golgi residents. The results could, therefore, indicate that Atgolgin-84 may act in concert with ERD2 to mediate the accumulation of soluble protein in the ER, but further work is required to specifically test this hypothesis.

Taken together, we suggest that Atgolgin-84A is located in a pre-*cis*-Golgi compartment, is involved in ER-Golgi tethering and potentially also Golgi-Golgi tethering, and may play an important function in the trafficking of proteins between the two first organelles of the secretory pathway.

Acknowledgements

References

Andreeva, A.V., Kutuzov, M.A., Evans, D.E. & Hawes, C.R. (1998) The structure and function of the Golgi apparatus: a hundred years of questions. *J. Exp. Bot.* **49**, 1281–1291.

Andreeva, A.V., Zheng, H., Kutuzov, M.A., Evans, D.E. & Hawes, C.R. (2000) Organization of transport from endoplasmic reticulum to Golgi in higher plants Plant ER and GA visualization with green fluorescent protein (GFP) Plant homologues of the proteins involved in ER-to-GA transport. *Biochem. Soc. Transac.*, 505–512.

Bascom, R.A., Srinivasan, S. & Nussbaum, R.L. (1999) Identification and characterization of golgin-84, a novel Golgi integral membrane protein with a cytoplasmic coiled-coil domain. *J. Biol. Chem.* **274**, 2953–2962.

Boevink, P., Oparka, K., Santa Cruz, S., Martin, B., Betteridge, A. & Hawes, C. (1998) Stacks on tracks: the plant Golgi apparatus traffics on an actin/ER network. *Plant J.* **15**, 441–447.

Brandizzi, F., Snapp, E.L., Roberts, A.G., Lippincott-Schwartz, J. & Hawes, C. (2002) Membrane protein transport between the endoplasmic reticulum and the Golgi in tobacco leaves is energy dependent but cytoskeleton independent: evidence from selective photobleaching. *Plant Cell* **14**, 1293–1309.

Chrispeels, M.J. & Herman, E.M. (2000) Endoplasmic reticulum-derived compartments function in storage and as mediators of vacuolar remodeling via a new type of organelle, precursor protease vesicles. *Plant Physiol.* **123**, 1227–1234.

Clough, S.J. & Bent, A.F. (1998) Floral dip: a simplified method for Agrobacterium-mediated transformation of *Arabidopsis thaliana. Plant J.* **16**, 735–743.

Da Costa, D.S., Pereira, S., Moore, I. & Pissarra, J. (2010) Dissecting cardosin B trafficking pathways in heterologous systems. *Planta* **232**, 1517–1530.

Da Silva, L.L., Snapp, E.L., Denecke, J., Lippincott-Schwartz, J., Hawes, C. & Brandizzi, F. (2004) Endoplasmic reticulum export sites and Golgi bodies behave as single mobile secretory units in plant cells. *Plant Cell* **16**, 1753–1771.

De, M., Lousa, C., Gershlick, D.C. & Denecke, J. (2012) Mechanisms and concepts paving the way towards a complete transport cycle of plant vacuolar sorting receptors. *Plant Cell* **24**, 1714–1732.

Diao, A., Rahman, D., Pappin, D.J., Lucocq, J. & Lowe, M. (2003) The coiled-coil membrane protein golgin-84 is a novel Rab effector required for Golgi ribbon formation. *J. Cell Biol.* **160**, 201–212.

Efimov, A., Kharitonov, A., Efimova, N. *et al.* (2007) Asymmetric CLASP-dependent nucleation of non centrosomal microtubules at the *trans*-Golgi network. *Dev. Cell* **12**, 917–930.

Foresti, O. & Denecke, J. (2008) Intermediate organelles of the plant secretory pathway: identity and function. *Traffic* **9**, 1599–1612.

Foresti, O., Gershlick, D.C., Bottanelli, F., Hummel, E., Hawes, C. & Denecke, J. (2010) A recycling-defective vacuolar sorting receptor reveals an intermediate compartment situated between prevacuoles and vacuoles in tobacco. *Plant Cell* **22**, 3992–4008.

Gilson, P.R., Vergara, C.E., Kjer-Nielsen, L., Teasdale, R.D., Bacic, A. & Gleeson, P.A. (2004) Identification of a Golgi-localised GRIP domain protein from *Arabidopsis thaliana. Planta* **219**, 1050–1056.

Goud, B. & Gleeson, P.A. (2010) TGN golgins, Rabs and cytoskeleton: regulating the Golgi trafficking highways. *Trends Cell Biol.* **20**, 329–336.

Hara-Nishimura, I., Shimada, T., Hatano, K., Takeuchi, Y. & Nishimura, M. (1998) Transport of storage proteins to protein storage vacuoles is mediated by large precursor-accumulating vesicles. *Plant Cell* **10**, 825–836.

Hawes, C. (2005) Cell biology of the plant Golgi apparatus. *New Phytol.* **165**, 29–44.

Hawes, C., Osterrieder, A. & Sparkes, I. (2008) Features of the plant Golgi apparatus. *The Golgi Apparatus* (ed. by A. A. Mironov & M. Pavelka). Springer, Vienna. 611–622.

Hawes, C. & Satiat-Jeunemaitre, B. (2005) The plant Golgi apparatus—going with the flow. *Biochim. Biophys. Acta* **1744**, 466–480.

Hawes, C., Schoberer, J., Hummel, E. & Osterrieder, A. (2010) Biogenesis of the plant Golgi apparatus. *Biochem. Soc. Trans.* **38**, 761–767.

Ito, Y., Uemura, T. & Nakano, A. (2018) The Golgi entry core compartment functions as a COPII-independent scaffold for ER-to-Golgi transport in plant cells. *J. Cell Sci.* **131**, pii: jcs203893.

Ito, Y., Uemura, T., Shoda, K., Fujimoto, M., Ueda, T. & Nakano, A. (2012) *cis*-Golgi proteins accumulate near the ER exit sites and act as the scaffold for Golgi regeneration after brefeldin A treatment in tobacco BY-2 cells. *Mol. Biol. Cell* **23**, 3203–3214.

Karimi, M., De Meyer, B. & Hilson, P. (2005) Modular cloning and expression of tagged fluorescent protein in plant cells. *Trends Plant Sci.* **10**, 103–105.

Kristen, U. (1978) Ultrastructure and a possible function of the intercisternal elements in dictyosomes. *Planta* **138**, 29–33.

Latijnhouwers, M., Gillespie, T., Boevink, P., Kriechbaumer, V., Hawes, C. & Carvalho, C.M. (2007) Localization and domain characterization of *Arabidopsis* golgin candidates. *J. Exp. Bot.* **58**, 4373–4386.

Latijnhouwers, M., Hawes, C., Carvalho, C., Oparka, K., Gillingham, A.K. & Boevink, P. (2005) An *Arabidopsis* GRIP domain protein locates to the *trans*-Golgi and binds the small GTPase ARL1. *Plant J.* **44**, 459–470.

Lowe, M. (2011) Structural organization of the Golgi apparatus. *Curr. Opin. Cell. Biol.* **23**, 85–93.

Malsam, J., Satoh, A., Pelletier, L. & Warren, G. (2005) Golgin tethers define subpopulations of COPI vesicles. *Science* **307**, 1095–1098.

March, W.B., Ram, P. & Gray, A.G. (2010) Fast euclidean minimum spanning tree: algorithm, analysis, and applications. In *Proceedings of the ACM SIGKDD International Conference on Knowledge Discovery and Data Mining*. Pp. 603–611.

Matheson, L.A., Hanton, S.L., Rossi, M., Latijnhouwers, M., Stefano, G., Renna, L. & Brandizzi, F. (2007) Multiple roles of ADP-ribosylation factor 1 in plant cells include spatially regulated recruitment of coatomer and elements of the Golgi matrix. *Plant Physiol.* **143**, 1615–1627.

Mathur, J., Mammone, A. & Barton, K.A. (2012) Organelle extensions in plant cells. *J. Integr. Plant Biol.* **54**, 851–867.

Moore, P.J., Swords, K.M.M., Lynch, M.A. & Staehelin, L.A. (1991) Spatial reorganization of the assembly pathways of glycoproteins and complex polysaccharides in the Golgi apparatus of plants. *J. Cell Biol.* **112**, 589–602.

Munro, S. (1995) An investigation into the role of transmembrane domains in Golgi protein retention. *EMBO J.* **14**, 4695–4704.

Munro, S. (2011) The golgin coiled-coil proteins of the Golgi apparatus. *Cold Spring Harb. Perspect. Biol.* **3**, a005256.

Osterrieder, A. (2012) Tales of tethers and tentacles: golgins in plants. *J. Microsc.* **247**, 68–77.

Osterrieder, A., Carvalho, C.M., Latijnhouwers, M., Johansen, J.N., Stubbs, C., Botchway, S. & Hawes, C. (2009) Fluorescence lifetime imaging of interactions between Golgi tethering factors and small GTPases in plants. *Traffic* **10**, 1034–1046.

Osterrieder, A., Hummel, E., Carvalho, C.M. & Hawes, C. (2009) Golgi membrane dynamics after induction of a dominant negative mutant Sar1 GTPase in tobacco. *J. Exp. Bot.* **61**, 405–422.

Osterrieder, A., Sparkes, I.A, Botchway, S.W., Ward, A., Ketelaar, T., De Ruijter, N.C.A & Hawes, C. (2017) Stacks off tracks: a role for the golgin AtCASP in plant endoplasmic reticulum-Golgi apparatus tethering. *J. Exp. Biol.* **68**, 3339–3350.

Pereira, C., Pereira, S., Satiat-Jeunemaitre, B. & Pissarra, J. (2013) Cardosin A contains two vacuolar sorting signals using different vacuolar routes in tobacco epidermal cells. *Plant J.* **76**, 87–100.

Preisinger, C., Short, B., De Corte, V., Bruyneel, E., Haas, A. & Kopajtich, R. (2004) YSK1 is activated by the Golgi matrix protein GM130 and plays a role in cell migration through its substrate 14-3-3zeta. *J. Cell Biol.* **164**, 1009–1020.

Ramirez, I.B. & Lowe, M. (2009) Golgins and GRASPs: holding the Golgi together. *Semin. Cell Dev. Biol.* **20**, 770–779.

Renka, R.J., Gebhardt, A. & Eglen, S. (2016) Tripack: Triangulation of Irregularly Spaced Data. http://www.R-project.org.

Renna, L., Hanton, S.L., Stefano, G., Bortolotti, L., Misra, V. & Brandizzi, F. (2005) Identification and characterization of AtCASP, a plant transmembrane Golgi matrix protein. *Plant Mol. Biol.* **58**, 109–122.

Saint-Jore, C.M., Evins, J., Batoko, H., Brandizzi, F., Moore, I. & Hawes, C. (2002) Redistribution of membrane proteins between the Golgi appa-

ratus and endoplasmic reticulum in plants is reversible and not dependent on cytoskeletal networks. *Plant J.* **29**, 661–678.

Satiat-Jeunemaitre, B., Cole, L., Bourett, T., Howard, R. & Hawes, C. (1996) Brefeldin A effects in plant and fungal cells: something new about vesicle trafficking? *J. Microsc.* **181**, 162–177.

Satoh, A., Wang, Y., Malsam, J., Beard, M.B. & Warren, G. (2003) Golgin-84 is a Rab1 binding partner involved in Golgi structure. *Traffic* **4**, 153–161.

Schoberer, J., König, J., Veit, C. *et al.* (2019) A signal motif retains Arabidopsis ER-α-mannosidase I in the *cis*-Golgi and prevents enhanced glycoprotein ERAD. *Nat. Commun.* **10**, 3701.

Schoberer, J., Runions, J., Steinkellner, H., Strasser, R., Hawes, C. & Osterrieder, A. (2010) Sequential depletion and acquisition of proteins during Golgi stack disassembly and reformation. *Traffic* **11**, 1429–1444.

Schoberer, J. & Strasser, R. (2011) Sub-compartmental organization of Golgi-resident N-glycan processing enzymes in plants. *Mol. Plant* **4**, 220–228.

Silva-Alvim, F.A.L., An, J., Alvim, J.C. *et al.* (2018) Predominant Golgi residency of the plant K/HDEL receptor is essential for its function in mediating ER retention. *Plant Cell* **30**, 2174–2196.

Sohda, M., Misumi, Y., Yamamoto, A. *et al.* (2010) Interaction of golgin-84 with the COG complex mediates the intra-Golgi retrograde transport. *Traffic* **11**, 1552–1566.

Sparkes, I.A., Ketelaar, T., De, Ruijter, N.C.A. & Hawes, C. (2009) Grab a Golgi: laser trapping of Golgi bodies reveals *in vivo* interaction with the endoplasmic reticulum. *Traffic* **10**, 567–571.

Sparkes, I., Runions, J., Kearns, A. & Hawes, C. (2006) Rapid, transient expression of fluorescent fusion proteins in tobacco plants and generation of stably transformed plants. *Nat. Protoc.* **1**, 2019–2025.

Staehelin, L.A. & Moore, I. (1995) The plant Golgi apparatus: structure, functional organisation and trafficking mechanisms. *Annu. Rev. Plant Physiol. Plant Mol. Biol.* **46**, 261–288.

Stefano, G., Renna, L., Chatre, L., Hanton, S.L., Moreau, P., Hawes, C. & Brandizzi, F. (2006) In tobacco leaf epidermal cells, the integrity of protein export from the endoplasmic reticulum and of ER export sites depends on active COPI machinery. *Plant J.* **46**, 95–110.

Sztul, E. & Lupashin, V. (2006) Role of tethering factors in secretory membrane traffic. *Am. J. Physiol. Cell Physiol.* **290**, C11–C26.

Takeuchi, M., Ueda, T., Sato, K., Abe, H., Nagata, T. & Nakano, A. (2000) A dominant negative mutant of Sar1 GTPase inhibits protein transport from the endoplasmic reticulum to the Golgi apparatus in tobacco and Arabidopsis cultured cells. *Plant J.* **23**, 517–525.

Thompson, J.D., Higgins, D.G. & Gibson, T.J. (1994) Clustal-W – improving the sensitivity of progressive multiple sequence alignment through sequence weighting, position-specific gap penalties and weight matrix choice. *Nucleic Acids Res.* **22**, 4673–4680.

Vieira, V., Peixoto, B., Costa, M., Pereira, S., Pissarra, J. & Pereira, C. (2019) N-linked glycosylation modulates Golgi-independent vacuolar sorting mediated by the plant specific insert. *Plants* **312**, pii: E312.

Vitale, A. & Denecke, J. (1999) The endoplasmic reticulum—gateway of the secretory pathway. *Plant Cell* **11**, 615–628.

Vitale, A. & Raikhel, N. (1999) What do proteins need to reach different vacuoles? *Trends Plant Sci.* **4**, 149–155.

Wang, P., Mugume, Y. & Bassham, D.C. (2018) New advances in autophagy in plants: regulation, selectivity and function. *Semin Cell Dev Biol.* **80**, 113-122.

Wang, X., Cai, Y., Wang, H., Zeng, Y., Zhuang, X., Li, B. & Jiang, L. (2014) *Trans*-Golgi network-located AP1 gamma adaptins mediate dileucine

motif-directed vacuolar targeting in Arabidopsis. *Plant Cell* **26**, 4102–4118.

Witte, K., Schuh, A.L., Hegermann, J. *et al.* (2011) TFG-1 function in protein secretion and oncogenesis. *Nat. Cell Biol.* **13**(5), 550–558.

Wong, M. & Munro, S. (2014) The specificity of vesicle traffic to the Golgi is encoded in the golgins coiled-coil proteins. *Science* **346**, 1256898.

Xiang, Y. & Wang, Y. (2011) New components of the Golgi matrix. *Cell Tissue Res.* **344**, 365–379.

Zeng, Y., Chung, K.P., Li, B. *et al.* (2015) Unique COPII component At-Sar1a/AtSec23a pair is required for the distinct function of protein ER export in *Arabidopsis thaliana*. *Proc. Natl. Acad. Sci. USA* **112**, 14360–14365.

Supporting Information

Additional supporting information may be found online in the Supporting Information section at the end of the article.

Figure S1: Quantification of Golgi tubules.
Figure S2: Tubule categories.
Figure S3: Movies showing that when a tethering event does not occur, the tubule does not come into contact with another Golgi body, instead it extends through the cytoplasm without attaching to another Golgi body and then collapses.